



Different determinants of radiation use efficiency in cold and temperate forests

Manuela Balzarolo^{1,2}  | Nadia Valdameri³ | Yongshuo H. Fu^{3,4}  | Lennert Schepers⁵ | Ivan A. Janssens³ | Matteo Campioli³

¹CSIC, Global Ecology Unit, CREAM-
CSIC-UAB, Cerdanyola del Vallès, 08913,
Catalonia, Spain

²CREAF, Cerdanyola del Vallès, 08193,
Catalonia, Spain

³Centre of Excellence Plants and Ecosystems
(PLECO), Department of Biology, University
of Antwerp, Wilrijk, 2610, Belgium

⁴College of Water Sciences, Beijing Normal
University, Beijing, 100875, China

⁵Ecosystem Management Research Group
(ECOB), Department of Biology, University
of Antwerp, Wilrijk, 2610, Belgium

Correspondence

Manuela Balzarolo, CSIC, Global Ecology
Unit, CREAM-CSIC-UAB, Cerdanyola del
Vallès, 08193, Catalonia, Spain; CREAM,
Cerdanyola del Vallès, 08193, Catalonia,
Spain.

Email: m.balzarolo@creaf.uab.cat

Funding information

H2020 Marie Skłodowska-Curie Actions,
Grant/Award Number: INDRO, grant no.
702717

Editor: Andrew Kerkhoff

Abstract

Aim: To verify which vegetation and environmental factors are the most important in determining the spatial and temporal variability of average and maximum values of radiation use efficiency (RUE_{ann} and RUE_{max} , respectively) of cold and temperate forests.

Location: Forty-eight cold and temperate forests distributed across the Northern Hemisphere.

Major taxa studied: Evergreen and deciduous trees.

Time period: 2000–2011.

Methods: We analysed the impact of 17 factors as potential determinants of mean RUE (at 8 days interval, annual and interannual level) and RUE_{max} (at annual and interannual level) in cold and temperate forests by using linear regression and random forests models.

Results: Mean annual RUE (RUE_{ann} , c. 1.1 gC/MJ) and RUE_{max} (c. 0.8 gC/MJ) did not differ between cold and temperate forests. However, for cold forests, RUE_{ann} was affected by temperature-related variables, while for temperate forests RUE_{ann} was affected by drought-related variables. Leaf area index (LAI) was important for both forest types, while N deposition only for cold forests and cloud cover only for temperate forest. RUE_{max} of cold forests was mainly driven by N deposition and LAI, whereas for temperate forests only a weak relationship between RUE_{max} and CO_2 concentration was found. Short-term variability of RUE was strongly related to the meteorological variables and varied during the season and was stronger in summer than spring or autumn. Interannual variability of RUE_{ann} and RUE_{max} was only weakly related to the interannual variability of the environmental drivers.

Main conclusions: Cold and temperate forests show different relationships with the environment and vegetation properties. Among the RUE drivers observed, the least anticipated was N deposition. RUE is strongly related to short-term and seasonal changes in meteorological variables among seasons and among sites. Our results

should be considered in the formulation of climate zone-specific tools for remote sensing and global models.

KEYWORDS

meteorological and vegetation influences, forest ecosystems, gross primary production, light use efficiency, meta-analysis, short-term variability, spatial and temporal variabilities

1 | INTRODUCTION

Radiation use efficiency (RUE; gC/MJ) has emerged in recent decades as a key parameter to determine photosynthetic carbon uptake by vegetation, and thus the carbon exchange between the atmosphere and biosphere (Monteith, 1972). RUE represents the efficiency of vegetation to transform absorbed light energy into organic compounds; it is the ratio between gross primary production (GPP; gC/m²/year) and the absorbed photosynthetically active radiation (APAR; MJ/m²/year), with APAR being the product of the incident photosynthetically active radiation (PAR; MJ/m²/year) and its fraction absorbed by vegetation (fAPAR) (Monteith, 1972):

$$\text{RUE} = \frac{\text{GPP}}{\text{APAR}} = \frac{\text{GPP}}{\text{fAPAR} \times \text{PAR}} \quad (1)$$

The global ecological modelling and the remote sensing communities are particularly interested in the RUE concept (e.g., Cheng, Zhang, Lyapustin, Wang, & Middleton, 2014; Grace et al., 2007; King, Turner, & Ritts, 2011; McCallum et al., 2009; Running et al., 2004; Stocker et al., 2018; Wang, Prentice, & Davis, 2014; Wang et al., 2017; Yuan et al., 2014). Nevertheless, to date, no consensus has been reached regarding the most suitable algorithm for RUE (Gitelson & Gamon, 2015) and scientists still need to fully understand if (and how) models should simulate the impact of environmental factors on RUE (Baldocchi, 2018). To do this, first we need to find suitable proxies that capture well RUE variability in space (from local to global) and in time (from daily to annual). RUE changes over time because GPP is affected by the current environmental conditions and because the absorbed radiation is affected by changes in incident PAR and leaf properties (e.g., leaf and chloroplast movement), which can occur over short time periods. On the other hand, the impact of respiration variability on RUE is expected to be low in the short term (when plant respiration is thought to be independent of photosynthesis) but it can be greater over longer, annual time-scales (when plant respiration is thought to be proportional to photosynthesis) (Ryan, Linder, Vose, & Hubbard, 1994).

First, RUE was used as a constant parameter (e.g., Myneni, Los, & Asrar, 1995). Subsequently, interannual variability has been recognized. The ratio between the accumulated GPP over the year and the total solar radiation absorbed by the canopy was then defined as annual RUE (RUE_{ann}). This definition has been widely used in simple crop growth models, based on in situ observations (McCallum et al., 2009), as well as in meta-analyses seeking general ecological elucidations (Fernández-Martínez et al., 2014). Finally, the intra-annual variability of RUE, due to its dependency on seasonal environmental

factors, was recognized (e.g., Grace et al., 2007). Production efficiency models define the light conversion factor as the product of an optimum RUE value (RUE potential or maximum, RUE_{max}) and other factors that relate to the environmental variables that regulate photosynthesis and APAR. For example, in the moderate resolution imaging spectroradiometer (MODIS) algorithm, RUE is implicitly calculated (to determine GPP) based on temperature, light, vapour pressure deficit and the biome-specific RUE_{max} derived from a look-up table (Zhao, Running, & Nemani, 2006). However, many studies considering different biomes (Garbulsky et al., 2010; Runyon, Waring, Goward, & Welles, 1994) have shown that RUE might be influenced not only by environmental factors, but also by a range of biophysical and structural factors related to plant properties, sometimes affected by ecosystem management (e.g., irrigation, fertilization). Both environmental and vegetation factors that affect RUE are reported in Table 1 with the aim of summarizing the current state of the art.

In detail, factors that have been reported to date as determinants of RUE are: (a) temperature-related variables [air and soil temperature, length of the warm period (i.e., the number of months with mean temperature above 5 °C), thermal amplitude (i.e., mean maximum minus mean minimum temperature)]; (b) water status variables [vapour pressure deficit (VPD), precipitation, intensity and duration of drought, evaporative fraction, actual and potential evapotranspiration, soil water content and deficit, irrigation]; (c) radiation-related variables [diffuse light and leaf area index (LAI)]; (d) variables related to leaf and vegetation characteristics [stand age, leaf habit and type and biome type] and (e) fertility-related variables [nitrogen (N) deposition, leaf N, management and CO₂ concentration]. The relevance of these factors is reviewed below based on the literature.

(a) Temperature-related variables. The impact of air temperature on RUE has been tested the most, but contrasting results have been found, ranging from significant (Chasmer et al., 2008; Kergoat, Lafont, Arneth, Dantec, & Saugier, 2008; Mäkelä et al., 2008; Schwalm et al., 2006) to non-significant (Jenkins et al., 2007; Turner et al., 2003), or with impact limited to periods during the warm season (see above definition; Fernández-Martínez et al., 2014) or only at cold sites (Garbulsky et al., 2010). The latter evidence is the most anticipated, as the positive effect of temperature on photosynthesis is larger in cold environments and APAR is not expected to depend significantly on temperature. Furthermore, Fernández-Martínez et al. (2014) tested the thermal amplitude and the length of the warm season, finding them not relevant to RUE variability.

(b) Water status variables. Water limitation is generally expected to reduce RUE because of reduced photosynthesis following reduction

TABLE 1 List of the vegetation and environmental drivers tested in the literature as potential drivers of radiation use efficiency (RUE) in forests

Potential RUE driver	Impact	Calculation of RUE				Level	Biome type(s)	Reference
		GPP	fAPAR, APAR	Annual or maximum	Study period			
<i>Cold forests</i>								
Soil water content	*	EC	RS	Annual	Growing season	Ecosystem	Forest: boreal (n = 4, chronosequence)	Chasmer et al. (2008)
Diffuse light	*							
Vapour pressure deficit	*							
Air temperature	*							
Stand age	*							
Canopy structure	*							
<i>Temperate forests</i>								
Fertilization	0	ANPP	I	Annual	Annual	Ecosystem	Forest: temperate (n = 2)	Allen et al. (2005)
Irrigation	*							
Diffuse light (diffuse : total radiation ratio)	*	EC	I	Annual	Growing season	Ecosystem	Forest: temperate (n = 1)	Jenkins et al. (2007)
Vapour pressure deficit	0							
Air temperature	0							
Soil temperature	0							
<i>Forest in different climate zones</i>								
Soil water content	*	ANPP	I	Annual	Annual	Ecosystem	Forest: temperate (n = 2)	Bracho et al. (2012)
Vapour pressure deficit	*							
Canopy structure (i.e., LAI), stand age	*							
Fertilization	0							
Fertilization	*	ANPP	P	Annual	Annual	Tree	Forest: temperate (n = 1)	Campoe et al. (2013)
Irrigation	0							
Fertilization + irrigation	*							
Tree size (effect of dominance)	*							
CO ₂ concentration	*	ANPP	I	Annual	Growing season	Ecosystem	Forest: temperate (n = 2)	De Kauwe et al. (2016)
<i>Forest in different climate zones</i>								
Diffuse light	*	EC	I	Annual	Growing season	Ecosystem	Forest: boreal (n = 1), temperate (n = 1), tropical (n = 1)	Alton, North, and Los (2007)
Canopy nitrogen	*	EC	I	Maximum RUE	Annual	Ecosystem	Forest: boreal (n = 3), temperate (n = 9)	Ollinger et al. (2008)
Leaf nitrogen	0	P	I	Annual	Annual	Ecosystem	Forest: boreal (n = 4), temperate (n = 3)	Mäkelä et al. (2008)
Air temperature	*							
Vapour pressure deficit	*							
Soil water content	0							

(Continues)

TABLE 1 (Continued)

Potential RUE driver	Calculation of RUE						Reference
	Impact	GPP	fAPAR, APAR	Annual or maximum	Study period	Level	
Canopy nitrogen	*	P	P	Maximum RUE	Annual	Leaf	Peltoniemi et al. (2012)
Vapour pressure deficit	0						
Air temperature	0						
Air temperature	*	EC	RS	Annual	Growing season	Ecosystem	Fernández-Martínez et al. (2014)
Actual evapotranspiration	0				Annual		
Precipitation	0				Annual		
Water deficit	0				Annual		
Thermal amplitude	0				Annual		
Length of warm period	0				Annual		
Nitrogen deposition	0				Annual		
Stand age	0				Annual		
Leaf habit and type	0				Annual		
Management	0				Annual		
<i>Forests and other biomes</i>							
Diffuse light	*	P	P	Annual	Growing season	Ecosystem	Gu et al. (2002)
Biome type	*	EC	I	Annual	Growing season	Ecosystem	Turner et al. (2003)
Diffuse light	*						
Vapour pressure deficit	0						
Air temperature max	0						
Biome type	*	EC	I	Annual	Annual	Ecosystem	Schwalm et al. (2006)
Leaf nitrogen	0						
Water cycle-related variables	*						
Diffuse light	*(n = 6)						
Air temperature	*						
LAI	*						
Evaporative fraction (water stress; moisture)	*(growing season)	EC	RS	Annual	Growing season	Ecosystem	Yuan et al. (2007)
Air temperature	*(begin and end of growing season)						

(Continues)

TABLE 1 (Continued)

Calculation of RUE									
Potential RUE driver	Impact	GPP	fAPAR, APAR	Annual or maximum	Study period	Level	Biome type(s)	Reference	
Leaf nitrogen	*	EC	I	Annual	Annual	Ecosystem	Forest: boreal (n = 12), temperate (n = 17), Mediterranean (n = 3) + tundra (n = 3) + grassland (n = 2) + cropland (n = 5)	Kergoat et al. (2008)	
Temperature	*								
Leaf nitrogen + air temperature	*								
Biome types	0								
Long-term mean annual precipitation	*	EC	RS	Annual	Annual	Ecosystem	Forest: boreal (n = 4), temperate (n = 10), Mediterranean (n = 3), tropical (n = 4) + tundra (n = 2) + shrubland (n = 1) + grassland (n = 7) + savanna (n = 3) + cropland (n = 1)	Garbulsky et al. (2010)	
Long-term mean annual temperature	0								
Precipitation	0								
Actual evapotranspiration	0								
Air temperature	0								
Biome types	0								
Long-term mean annual precipitation	0	EC	RS	Maximum RUE	Annual	Ecosystem	See row above	Garbulsky et al. (2010)	
Long-term mean annual temperature	0								
Precipitation	*								
Air temperature	0								
Actual evapotranspiration	0								
Biome types	0								
Biome types	*	EC	RS	Annual	Growing season	Ecosystem	See two rows above	Garbulsky et al. (2010)	
Air temperature	0								
Vapour pressure deficit	0								
Evaporative fraction	*								
AET/PET	0								
Precipitation	0								

Symbols: * = significant impact; 0 = no significant impact.

Abbreviations: Potential drivers: LAI = leaf area index; AET = actual evapotranspiration; PET = potential evapotranspiration. Variables used to calculate RUE: GPP = gross primary production (measurement methods of GPP); EC = eddy covariance; ANPP = measurements based on aboveground net primary productivity; P = simulated by processed based models; APAR: absorbed photosynthetically active radiation; fAPAR: fraction of APAR; (measurement methods of fAPAR: I = derived from in situ optical LAI or radiation measurements; P = simulated by processed based models; RS = derived from satellite data).

in stomatal conductance or stomata closure. VPD has frequently been tested as a potential driver of RUE. As can be seen in Table 1, both significant (Bracho et al., 2012; Chasmer et al., 2008; Mäkelä et al., 2008; Runyon et al., 1994) and non-significant (Garbulsky et al., 2010; Jenkins et al., 2007; Turner et al., 2003) impacts of VPD on RUE have been found. Also annual precipitation was identified both as a significant (Garbulsky et al., 2010) and a non-significant driver of RUE (Fernández-Martínez et al., 2014). In the latter work, the water deficit was tested as potential driver of RUE (i.e., an indicator of the intensity of water stress that the vegetation must tolerate) but with a negative response. Soil water content was reported as a significant driver of RUE in one study on temperate forests (Bracho et al., 2012) and one on cold forests (Chasmer et al., 2008), while it was not relevant in the study of Mäkelä et al. (2008), comparing cold and temperate forests. The evaporative fraction was found to be a significant driver by Garbulsky et al. (2010) and Yuan et al. (2007). Actual evapotranspiration was identified as an important variable by Garbulsky et al. (2010), but not by Fernández-Martínez et al. (2014). Two irrigation experiments on temperate forests (Allen, Will, McGarvey, Coyle, & Coleman, 2005; Campoe et al., 2013) both agreed on the potential influence of irrigation on RUE.

(c) *Radiation-related variables.* The role of diffuse light has been tested in several studies, focused only on forests or combining forests with other biomes (Table 1). All studies agreed on its potential role in defining RUE variability because the reduction that the diffuse light triggers in APAR is larger than the reduction it triggers in GPP (Gu et al., 2002). The APAR term in Monteith's model depends not only on the amount of PAR, but also on the PAR absorbance capacity, and thus canopy structure, leaf area index (LAI) (Bracho et al., 2012; Schwalm et al., 2006), leaf angle distribution and photosynthetic pigment content.

(d) *Variables related to leaf and ecosystem characteristics.* Stand age, leaf habitat and type, and biome types have been tested as potential drivers of RUE. Stand age has been identified both as a significant (Bracho et al., 2012; Chasmer et al., 2008) and non-significant driver of RUE (Fernández-Martínez et al., 2014), whereas leaf habitat and type were found to be non-significant (Fernández-Martínez et al., 2014). It has been reported by several authors that RUE varies with vegetation type (Field, Randerson, & Malmstrom, 1995; Garbulsky et al., 2010; Prince & Goward 1995; Schwalm et al., 2006; Turner et al., 2003) because of the different ratio of respiration to photosynthesis. RUE was found to be around 2 gC/MJ for annual crops, for which the ratio of respiration to photosynthesis is assumed to be low, whereas for woody plants the value of RUE varies from 0.2 to 1.5 gC/MJ because the ratio of respiration to photosynthesis is assumed to increase with plant size (Hunt, 1994; Waring & Running, 1998).

(e) *Fertility-related variables.* The impact of fertility on RUE has been tested in two experiments on temperate forests but contrasting results were found [significant in Campoe et al. (2013), non-significant in Allen et al. (2005)]. Bracho et al. (2012) identified fertility as not influential for RUE in drought conditions. Leaf nitrogen content affects RUE directly (mainly through its impact on photosynthesis)

but also indirectly (through its impact on leaf and plant structure, which influence light absorption). Leaf N has been therefore considered as a potential driver of RUE in manifold studies on forest ecosystems (Kergoat et al., 2008; Ollinger et al., 2008; Peltoniemi et al., 2012) but has not been found to be consistently significant (Mäkelä et al., 2008; Schwalm et al., 2006). In a recent study, Fernández-Martínez et al. (2014) tested the relationship between RUE and N deposition but no significant association was found. Finally, De Kauwe, Keenan, Medlyn, Prentice, and Terrer (2016) have recently shown that CO₂ is a key factor controlling RUE variability. These authors found a large increase in RUE due to elevated CO₂ for two long-term free air carbon enrichment (FACE) forest sites (Oak Ridge: 1998–2008 and Duke: 1996–2007).

Overall, even though the underlying mechanisms for the different potentially influencing factors seem clear, our literature review indicates that there is still high uncertainty about the vegetation and environmental drivers of RUE, their relative importance and their different impacts on forest ecosystems of different climate zones. Moreover, the biological and physiological processes that regulate photosynthesis and radiation absorption vary daily over the growing season and, potentially, among years. Therefore, here, we aim to elucidate the spatial (across the Northern Hemisphere) and temporal (short-term, annual and interannual) variability of RUE in temperate and cold forests by comparing the impact on RUE and RUE_{max} of several potential drivers. The short-term variability refers to the variability of RUE among 8-day time windows (RUE_{8days}), as 8 days is a common time reference for remote sensing. The focus on RUE_{8days}, RUE_{ann} and RUE_{max} offers the most comprehensive insight into RUE dynamics and their possible implementation in global monitoring tools.

2 | MATERIALS AND METHODS

2.1 | Forest categories and sites

It appears clear that most of the variables (e.g., related to temperature, water status, fertility) potentially affecting RUE differ between the two main climate zones where the majority of the northern forests are situated, that is, the temperate and cold zones. As for most of the previous studies on RUE variability (see Table 1), we therefore separated the two forest types in our analysis. This categorization is also important to generalize our findings and match the forest land classification used in global vegetation modelling.

The categorization of cold and temperate is based on the Köppen–Geiger classification (Peel, Finlayson, & McMahon, 2007), using monthly temperature data from the European Commission–Joint Research Centre–Monitoring Agricultural ResourceS (EC-JRC-MARS, <https://ec.europa.eu/jrc/en/mars>) portal. The Köppen–Geiger classification defines a particular site as “cold” when the temperature of the hottest month is > 10°C, while the temperature of the coldest month is below or equal to 0°C. On the other hand, sites are classified as “temperate” when the temperature of

the hottest month is $> 10^{\circ}\text{C}$ and the temperature of the coldest month is between 0 and 18°C .

For the analysis on spatial variability of RUE_{ann} we used 26 cold and 22 temperate forests in the Northern Hemisphere (Figure 1). These sites were selected because they had both GPP derived from eddy covariance flux measurements and the associated satellite value of fAPAR available (see below for fAPAR determination). Multiple years were considered when available. Total site-year combinations were 114 for cold and 102 for temperate forests (see Supporting Information Appendix S1). For the analysis of the spatial variability of RUE_{max} , only the sites with seasonal data for GPP and fAPAR were selected. A subset of 20 cold forests and 20 temperate forests was thus used (see Supporting Information Appendix S1). The temporal analyses (interannual variability of RUE_{ann} and RUE_{max} and short-term RUE variability, $\text{RUE}_{8\text{days}}$) were conducted by considering 11 sites that had at least 8 years of seasonal data for GPP and fAPAR.

2.2 | PAR, fAPAR, GPP and RUE

PAR. The cumulative annual value of PAR (PAR_{ann}) and 8-day PAR ($\text{PAR}_{8\text{days}}$) were calculated, for every site-year combination, from seasonal daily data for PAR using (a) free fair-use data files from the Fluxnet and European Fluxes Database Cluster (69% of the sites) and (b) the EC-JRC-MARS data set for the remaining sites. (a) In the Fluxnet and European Fluxes Database Cluster files the measurement of the incoming radiation in the PAR region (400–700 nm) is reported. (b) EC-JRC-MARS reports only total shortwave incoming radiation. We therefore multiplied the radiation by a factor of 0.45, assuming that

about 45% of the total incoming shortwave radiation is in the PAR region (Campbell & Norman, 1998). The physical unit of the total shortwave radiation reported in the EC-JRC-MARS database is $\text{MJ}/\text{m}^2/\text{day}$. The physical unit of incoming PAR in the Fluxnet and European Flux Database Cluster is $\mu\text{mol}/\text{photons}/\text{m}^2/\text{s}$. We converted PAR from $\mu\text{mol}/\text{photons}/\text{m}^2/\text{s}$ to $\text{J}/\text{m}^2/\text{s}$ using a conversion factor of $4.55 \mu\text{mol}/\text{J}$ as proposed by Goudriaan and Van Laar (1994). Finally, we obtained daily values in $\text{MJ}/\text{m}^2/\text{day}$ by multiplying by 0.0864. For sites with availability of both, preliminary analyses indicated a high correlation between PAR data from EC-JRC-MARS and the Fluxnet/ European Fluxes Database Cluster ($R^2 = .8$; $p < .001$; slope = 1.05).

fAPAR. 8-day values of fAPAR ($\text{fPAR}_{8\text{days}}$) were derived from the fAPAR/LAI product (MOD15A2, collection 5) from the MODIS/TERRA satellite sensor/platform as provided by the Oak Ridge National Laboratory Distributed Active Archive Center (ORNL DAAC). MOD15A2 pixel values represent the optimal $\text{fPAR}_{8\text{days}}$ at 1-km spatial resolution (Myneni et al., 2002). Only the pixels with the highest quality based on the Quality Assurance/Quality Control flags provided by MODIS (e.g., clear conditions without snow) were selected and retained for computing fAPAR values. For each year, annual fAPAR ($\text{fAPAR}_{\text{annW}}$) was calculated from weighted $\text{fPAR}_{8\text{days}}$ data where the weighting was provided by $\text{PAR}_{8\text{days}}$ data.

APAR. Annual APAR (APAR_{ann}) was computed as $\text{fAPAR}_{\text{annW}}$ multiplied by the cumulative PAR (PAR_{ann}). To derive $\text{APAR}_{8\text{days}}$, we multiplied $\text{fAPAR}_{8\text{days}}$ by the $\text{PAR}_{8\text{days}}$.

GPP. GPP data (annual cumulative GPP) and 8-day GPP ($\text{GPP}_{8\text{days}}$) were derived from publicly available databases of forest ecosystem carbon fluxes (Luyssaert et al., 2007, Fluxnet, European Flux Database Cluster).

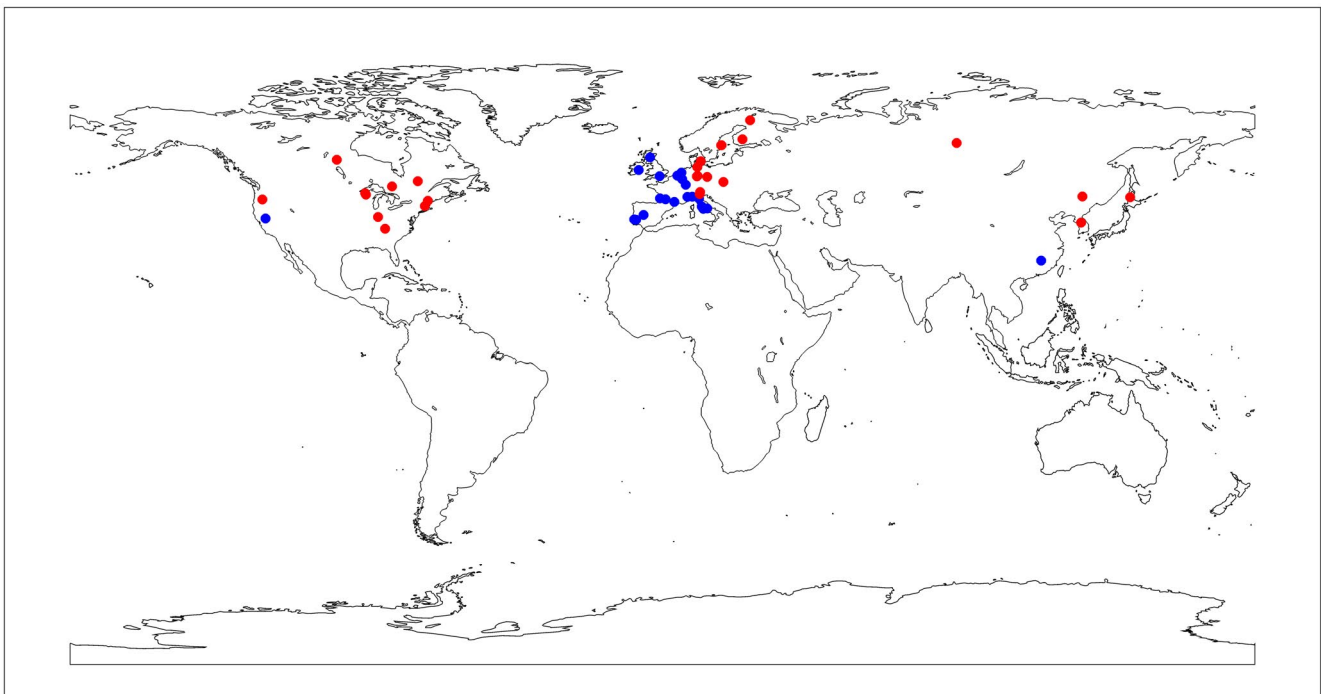


FIGURE 1 Map with distribution of sites: cold forests and temperate forests are represented with red and blue circles, respectively [Colour figure can be viewed at wileyonlinelibrary.com]

RUE_{ann} , RUE_{max} and RUE_{8days} . According to Monteith's equation (Equation 1), we calculated RUE_{ann} as the ratio between GPP_{ann} and $APAR_{ann}$. To calculate RUE_{max} for a year we computed 8-day RUE (RUE_{8days}) values for the whole growing season from the ratio between GPP_{8days} and $APAR_{8days}$ values. RUE_{max} was defined as the maximum value of the RUE_{8days} time series.

2.3 | Explanatory drivers

2.3.1 | Analyses of spatial variability

We examined the following potential determinants of RUE_{ann} and RUE_{max} that were in common with previous studies: leaf type and habit, annual potential evapotranspiration, annual precipitation, mean annual temperature, mean monthly minimum and maximum air temperature, N deposition, VPD, cloud cover data, LAI, aridity index, leaf N and CO_2 concentration. Furthermore, we decided to complete the group of determinants with the addition of some new variables related to soil fertility, number of days with mean daily temperature below zero (i.e., freezing period) and duration of the longest period without rain. These variables were determined for each site and year for which RUE_{ann} was available, except for LAI and leaf N concentration, for which data were not consistently available for all years (averages were made with the available data) or sites (leaf N concentration was available only at about half of the sites and only those sites were considered in the data analysis for leaf N).

2.3.2 | Analyses of temporal variability

For the analysis of short-term variability of RUE_{8days} the available (meteorological) variables were: mean 8-day temperature, 8-day minimum and maximum temperature, 8-day mean potential evapotranspiration, 8-day mean VPD and 8-day mean CO_2 concentration. For the analysis of the interannual variability of both RUE_{ann} and RUE_{max} , we considered the same meteorological explanatory variables used for the analysis of short-term variability of RUE_{8days} .

(a) Meteo-variables

Mean annual temperature, mean monthly minimum and maximum temperature, annual precipitation and potential evapotranspiration, yearly number of days with mean daily temperature below zero and the duration of the longest period without rain (expressed in number of days), mean 8-day temperature, 8-day minimum and maximum temperature, 8-day mean potential evapotranspiration and 8-day mean VPD were calculated using the EC-JRC-MARS data set. The evaporation data that we used are derived from Penman (1948) and they represented the annual potential evapotranspiration. We calculated the annual aridity index as the ratio of annual precipitation to annual evapotranspiration.

VPD (in kPa) is the difference between the saturation vapour pressure (e_s , kPa) at air temperature and actual vapour pressure (e_a , kPa) (Allen, Pereira, Raes, & Smith, 1998):

$$VPD = e_s - e_a \quad (2)$$

$$e_s = 0.6108 \exp\left(\frac{17.27T}{T + 237.3}\right) \quad (3)$$

$$e_a = e_s \frac{RH}{100} \quad (4)$$

where T is the air temperature ($^{\circ}C$) and RH is the relative humidity (%). Mean daily values of VPD over an 8-day time window and the annual mean of daily values were used in our analyses. RH data were available from the Fluxnet and European Fluxes Database Cluster for 89% of the sites, while for the other sites we used data from the public online Global Weather Data for soil & water assessment tool (SWAT) (Dile & Srinivasan, 2014; Fuka et al., 2014) that provides interpolated RH from local meteorological stations.

Cloud cover was used as a proxy of diffuse light, as the latter is a parameter that is not generally measured by meteorological stations and flux towers. We extracted cloud cover data (mean annual value as percentage) from Climatic Research Unit (CRU) Time-Series Version 3.22 (Harris & Jones, 2014).

(b) Soil fertility

The soil type of each site was derived from the food and agriculture organization (FAO) digital Soil Map of the World Version 3.6 (FAO, 2007). Subsequently, soil types were classified into three levels (H: high, M: medium, L: low) of nutrient availability (see Supporting Information Appendix S1), based on fertility information reported in Creutzberg (1987).

(c) Leaf type and habit

We collected the description of each site from the database of Luysaert et al. (2007). The two leaf type categories are needle-leaved and broadleaved, while the categories deciduous and evergreen represent the leaf habit of the forest tree species.

(d) N deposition

In our analysis, N deposition was considered as the sum of dry and wet deposition. We extracted these data from the global N deposition data set simulated with goddard earth observing system-Chem (GEOS; <http://acmg.seas.harvard.edu/geos/index.html>) for years from 2004 to 2006, at $2^{\circ} \times 2.5^{\circ}$ grid resolution (Ackerman, Chen, & Millet, 2018).

(e) LAI and leaf N concentration

We extracted LAI data from the forest database of Luysaert et al. (2007) and the literature (see Supporting Information Appendix S2). Leaf N was obtained from the ancillary files of the Fluxnet and European Fluxes Database Cluster and the literature (see Supporting Information Appendix S3). For both LAI and leaf N concentration, we used the maximum annual value.

(f) CO_2 concentration

For 81% of the sites, we used CO_2 concentration data from the Fluxnet database. For the remaining sites, we used values provided

in the global data set compiled by the Institute for Atmospheric and Climate Science at the Eidgenössische Technische Hochschule in Zürich (Switzerland) for the Northern Hemisphere (<https://www.co2.earth/historical-co2-datasets>).

2.4 | Statistical analysis

2.4.1 | Spatial variability of RUE_{ann} and RUE_{max}

The analyses of RUE_{ann} and RUE_{max} were conducted separately for cold forests and temperate forests (see Tables 2 and 3), with the analysis on the entire data set reported only in the Supporting Information (see Appendices S4 and S5). Three main analyses were performed: univariate analysis, random forest and linear models with multiple predictors. Analyses on leaf N were limited to the univariate analysis (see below), because we did not have leaf N available for all sites (see above). (a) To describe the correlation between each predictor and RUE_{ann} and RUE_{max} , we conducted univariate analysis for each variable. We used single linear regression for continuous variables and one-way ANOVAs with post hoc Tukey's honestly significant difference (HSD) test for categorical variables. Shapiro–Wilk's normality test and Levene's test for homoscedasticity were always passed. (b) We used random forest analysis (Breiman, 2001) to estimate the relative importance of the different variables. This analysis ranks the factors from the one with the strongest impact to the one with the lowest impact, while not exclusively considering linearity but also other, nonlinear, types of relationships. The ranking is based on the mean decrease in accuracy of model prediction (%IncMSE) when the variable is randomly permuted. We used a standard random forest algorithm (Liaw & Wiener, 2002) with 50,000 trees. For ranking the predictors, we preferred random forest to multiple regression analysis because of the ability of random forest analysis to consider also nonlinear relationships and because the relatively small sample sizes would have made the ranking with multiple regression analysis less robust. (c) Finally, we built linear models with the predictors to evaluate how much of the variability in RUE could be explained by combinations of predictors. To build these models, we first detected the variables that were highly correlated by doing a multicollinearity test [recording the variance inflation factor (VIF)] and by exploring the relationships among all the variables with a bivariate analysis by doing a matrix of Pearson's correlation coefficients. Practically, we removed all variables that had a VIF > 5 or had a correlation coefficient > |.8| with another variable. With the variables that passed the multicollinearity and correlation test, we performed a stepwise backwards regression analysis (SBRA). This is a process of building a model considering at first all variables together and successively removing the least important ones. The original model was compared with the new model, with one variable removed, by using the likelihood ratio and Akaike information criterion (AIC). The new model was not accepted if the likelihood ratio was significant ($p < .05$) or the AIC increased (i.e., we considered as the final model the one that respected those assumptions).

2.5 | Temporal analysis of short-term RUE variability

For this test, we performed univariate analyses considering as dependent variable the time series of RUE_{8days} and as independent variables the 8-day time series of the predictors (see above). The analyses were done for each of the 11 selected sites, separately, and averages were done across years. First, the analyses were done for all 8-day periods within the growing season. Second, the analyses were run separately for three periods representing the main seasons: spring (considering 8-day windows from 15 April to 15 June), summer (from 16 June to 15 August) and autumn (from 16 August to 15 October).

2.5.1 | Temporal analysis of interannual variability of RUE_{ann} and RUE_{max}

This analysis was done separately on the selected 11 sites (see above). We conducted a univariate analysis to evaluate the goodness of the linear correlation between RUE (RUE_{ann} and RUE_{max}) of each year and the value of each predictor variable (see above for the variables list). For RUE_{ann} , we used annual values of the predictor variables. For predictors of RUE_{max} , we used the values of the 8-day window corresponding to the 8-day period associated with RUE_{max} .

All the statistical analyses were done using R (R Core Team, 2015).

3 | RESULTS

Mean RUE_{ann} for cold and temperate forests was very similar: 1.10 ($SD \pm 0.39$) gC/MJ for cold forests and 1.11 ($SD \pm 0.45$) gC/MJ for temperate forests. The variability of RUE_{ann} was larger than the variability of annual GPP [1,221.46 ($SD \pm 412.60$) gC/m²/year and 1,510.27 ($SD \pm 329.53$) gC/m²/year for cold and temperate forests, respectively]. Cold forests showed the largest RUE_{max} but also the largest variability across sites [0.86 ($SD \pm 0.42$) gC/MJ], whereas temperate forests presented slightly lower values [0.79 ($SD \pm 0.26$) gC/MJ].

The results of the univariate analyses are shown in Tables 2 and 3 for RUE_{ann} and RUE_{max} , respectively, for both cold and temperate forests. For cold forests, temperate-related variables were significantly correlated with RUE_{ann} , in particular the number of days with mean daily temperature below zero ($p = .001$, $R^2 = .35$), annual temperature ($p = .03$, $R^2 = .14$) and, but with a weaker trend, Tmin ($p = .06$, $R^2 = .11$). Moreover, N deposition ($p = .02$, $R^2 = .18$) and LAI ($p = .05$, $R^2 = .12$) were also significant determinants of spatial variability of RUE_{ann} (Table 2). On the other hand, RUE_{max} showed a significant relationship only with N deposition ($p = .02$, $R^2 = .20$) and LAI ($p = .05$, $R^2 = .16$) and only a weak relationship with temperature (Tmin; $p = .07$; $R^2 = .13$) (Table 3). For temperate forests, a different picture emerged. First, RUE_{ann} showed dependencies with variables related to the water status instead of temperature,

TABLE 2 The impact of vegetation and environmental drivers on annual radiation use efficiency (RUE_{ann}) for cold ($n = 26$) and temperate forests ($n = 22$), from univariate analysis and stepwise backwards regression analysis (SBRA)

Potential predictor	Cold forest ($n = 26$)					Temperate forest ($n = 22$)			
	Variable type ^a	Univariate analysis ^b				Univariate analysis ^b			
		p value	Adj. R^2 (sign)	Post hoc	SBRA ^c	p value	Adj. R^2 (sign)	Post hoc	SBRA ^c
<i>Water-related</i>									
Aridity index	con.	.73	-.04 (-)		X	.003**	.34 (+)		X
Longest period without rain	con.	.78	-.04 (-)		X	.01*	.23 (-)		X
Annual precipitation	con.	.72	-.04 (+)		X	.02*	.19 (+)		
Evapotranspiration	con.	.62	-.03 (+)		X	.56	-.03 (-)		X
Vapour pressure deficit	con.	.34	-.003 (+)			.05 ^o	.13 (-)		X
<i>Temperature-related</i>									
Number days under 0°C	con.	.001**	.35 (-)		X	.27	.01 (+)		
Annual temperature	con.	.03*	.14 (+)			.16	.05 (-)		X
Tmin	con.	.06 ^o	.11 (+)		X	.25	.02 (-)		X
Tmax	con.	.99	-.04 (+)		X	.13	.06 (-)		X
<i>Radiation-related</i>									
Cloud cover data	con.	.93	-.04 (+)			.002**	.34 (+)		X
LAI	con.	.05 ^o	.12 (+)			.01*	.24 (+)		X
<i>Others</i>									
N deposition	con.	.02*	.18 (+)			.1	.09 (+)		
Soil fertility ^d	cat.	.23		L-H: -0.30		.38		M-H: -0.35	X
Leaf habit ^e	cat.	.2		BN-B: -0.26		.36		BN-B: 0.27	
Leaf type ^f	cat.	.28		E-D: -0.27		.74		E-D: -0.12	
Leaf N ^g	con.	.39	-.01 (+)			.36	.001 (+)		
CO ₂	con.	.73	-.04 (-)			.21	.03 (+)		
Stepwise backwards regression model						$R^2 = .57$			$R^2 = .38$

Abbreviations and symbols: LAI = leaf area index; Tmin and Tmax = mean monthly minimum and maximum air temperature, respectively; Number days under 0°C = the number of days in a year with mean daily temperature below zero. ^o = .05 < p < .10; * = .01 < p < .05; ** = .001 < p < .01; *** = p < .001; (+) = positive linear regression; (-) = negative linear regression. ^aVariable type: "con." when continuous; "cat." when categorical. ^bFor continuous variables, the significance level of the linear regression (p) and adjusted R^2 are reported, with "sign" as the sign of the linear regression. For categorical variables, we report results of one-way ANOVA (p value) and post hoc Tukey's honestly significant difference (HSD) test (absolute difference for two significantly different factors and p value of the difference). ^cFor SBRA, we report the variables of the final model, representing the key predictors of RUE, and (in the last row) the coefficient of determination (R^2) of the final model; ^dSoil fertility was classified as H = high; M = medium; L = low. ^eLeaf habit was classified as N = needleleaved; B = broadleaved; BN = mixed habit. ^fLeaf type was classified as D = deciduous; E = evergreen. ^gLeaf N: variable tested only for univariate analysis as with fewer sites than other variables (cold: $n = 11$; temperate: $n = 12$).

in particular annual precipitation ($p = .02$, $R^2 = .19$), aridity index ($p = .003$, $R^2 = .34$), longest period without rain ($p = .01$, $R^2 = .23$) and VPD ($p = .05$, $R^2 = .13$) (Table 2). Second, RUE_{ann} of temperate forests showed mainly different patterns from those of RUE_{ann} of cold forests such as a significant relationship with cloud cover ($p = .002$, $R^2 = .34$) and a non-significant relationship with N deposition ($p = .62$, $R^2 = -.04$) (Table 2). Finally, RUE_{max} of temperate forests did not show significant relationships with any explanatory variable

except a weak relationship with CO₂ concentration ($p = .09$, $R^2 = .10$) (Table 3).

In general, there was a good agreement between the univariate analysis and random forest analysis and the variables that were significant in the univariate analysis also showed high importance in the random forest analysis (Figures 2 and 3). However, there were exceptions. First, for temperate forests, the relation between RUE_{ann} and maximum air temperature was not significant according to the

TABLE 3 The impact of vegetation and environmental drivers on maximum radiation use efficiency (RUE_{max}) for cold ($n = 20$) and temperate forests ($n = 20$), from univariate analysis and stepwise backwards regression analysis (SBRA)

Potential predictor	Variable type ^a	Cold forest ($n = 20$)				Temperate forest ($n = 20$)			
		Univariate analysis ^b				Univariate analysis ^(b)			
		p value	Adj. R^2 (sign)	Post hoc	SBRA ^c	p value	Adj. R^2 (sign)	Post hoc	SBRA ^c
<i>Water-related</i>									
Aridity index	con.	.23	.03 (+)		X	.26	.02 (+)		X
Longest period without rain	con.	.36	-.01 (-)		X	.11	.09 (-)		X
Annual precipitation	con.	.20	.04 (+)		X	.56	-.04 (+)		X
Evapotranspiration	con.	.79	-.05 (+)		X	.55	-.03 (-)		X
Vapour pressure deficit	con.	.91	-.05 (+)		X	.45	-.02 (-)		X
<i>Temperature-related</i>									
Number days under 0°C	con.	.13	.08 (-)		X	.80	-.05 (+)		X
Annual temperature	con.	.14	.07 (+)		X	.40	-.01 (-)		
Tmin	con.	.07 ^o	.13 (+)		X	.50	-.03 (-)		X
Tmax	con.	.91	-.05 (-)		X	.55	-.03 (-)		X
<i>Radiation-related</i>									
Cloud cover data	con.	.93	-.06 (+)		X	.23	.03 (+)		X
LAI	con.	.05*	.16 (+)			.20	.04 (+)		X
<i>Others</i>									
N deposition	con.	.02*	.20 (+)		X	.62	-.04 (+)		X
Soil fertility ^d	cat.			L-H: 0.77	X			L-H: 0.36	X
Leaf habit ^e	cat.			BN-B: 0.49				BN-B: 0.91	X
Leaf type ^f	cat.			E-D: 0.49				E-D: 0.47	X
Leaf N ^g	con.	.79	-.10 (-)			.29	.02 (+)		
CO ₂ concentration	con.	.80	-.05 (-)		X	.09 ^o	.10 (+)		
Stepwise backwards regression model									$R^2 = .88$

Abbreviations and symbols: LAI = leaf area index; Tmin and Tmax = mean monthly minimum and maximum air temperature, respectively; Number days under 0°C = the number of days in a year with mean daily temperature below zero. ^o = .05 < p < .10; * = .01 < p < .05; ** = .001 < p < .01; *** = p < .001. (+): positive linear regression; (-): negative linear regression. ^aVariable type: "con." when continuous; "cat." when categorical. ^bFor continuous variables, the significance level of the linear regression (p) and adjusted R^2 are reported, with "sign" as the sign of the linear regression. For categorical variables, we report results of one-way ANOVA (p value) and post hoc Tukey's honestly significant difference (HSD) test (absolute difference for two significantly different factors and p value of the difference). ^cFor SBRA, we report the variables of the final model, representing the key predictors of RUE, and (in the last row) the coefficient of determination (R^2) of the final model. ^dSoil fertility was classified as H = high; M = medium; L = low. ^eLeaf habit was classified as N = needleleaved; B = broadleaved; BN = mixed habit. ^fLeaf type was classified as D = deciduous; E = evergreen. ^gLeaf N = variable tested only for univariate analysis as with fewer sites than other variables (cold: $n = 11$; temperate: $n = 12$).

univariate analysis but was highly ranked in random forest analysis (see Figure 2 and Table 2). This is probably due to the hyperbolic relationship between maximum temperature and RUE_{ann} which was likely detected by the random forest but not by the univariate analysis (Supporting Information Appendix S6). However, we believe this relationship to be spurious as it is driven by only three sites with exceptionally high maximum temperatures (Supporting Information Appendix S6). Second, similarly to the previous case, RUE_{max} of cold forests was not significantly correlated with Tmean in the univariate

analysis but Tmean was highly ranked in the random forest analysis, likely because of a few exceptional sites (Supporting Information Appendix S7). Third, for RUE_{ann} and RUE_{max} of cold forests, LAI was significant according to the univariate analysis but of very low importance in the random forest analysis. This suggests that for RUE_{ann} and RUE_{max} of cold forests, nonlinear relationships might dominate and overshadow the linear dependencies.

Tables 2 and 3 also show linear models combining multiple predictors. The models explained 57 and 38% of the spatial variability of

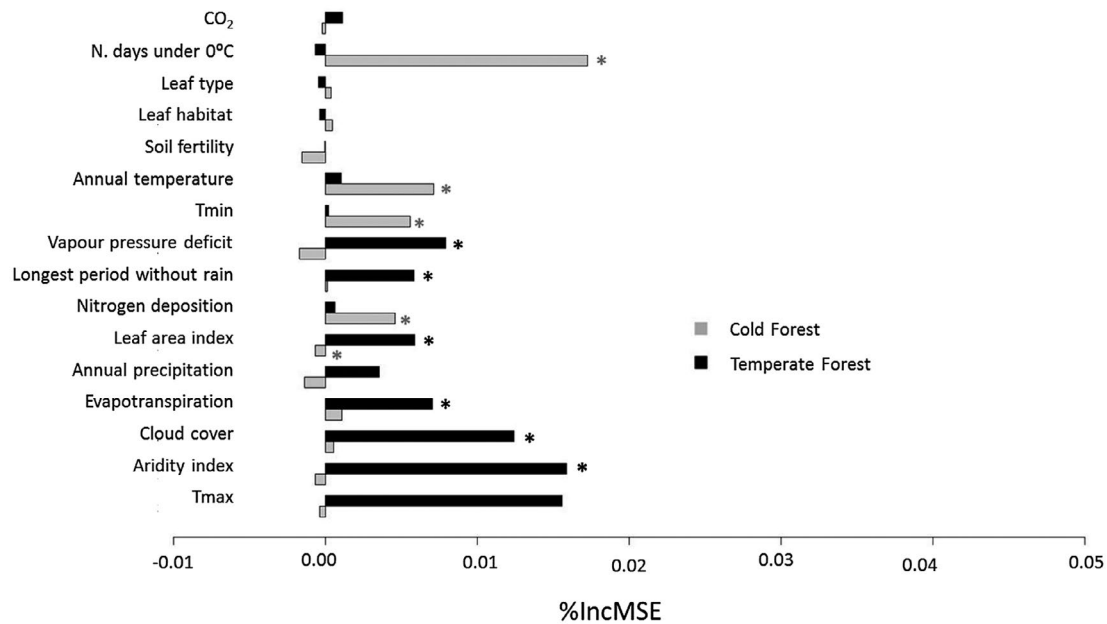


FIGURE 2 Relative importance of vegetation and environmental drivers for annual radiation use efficiency (RUE_{ann}) for cold forests ($n = 26$) and temperate forests ($n = 22$). Data are from (a) random forest analysis (cold forests: light grey bars, temperate forests: black bars) with variable importance positively related to accuracy of model prediction (%IncMSE), and negative %IncMSE indicating lack of importance and (b) univariate analysis, with significant ($p < .10$) drivers marked with "*" symbol (see text and Table 2 for details). Abbreviations: Tmin and Tmax = mean monthly minimum and maximum air temperature, respectively; N. days under 0°C = the number of days in a year with mean daily temperature below 0°C

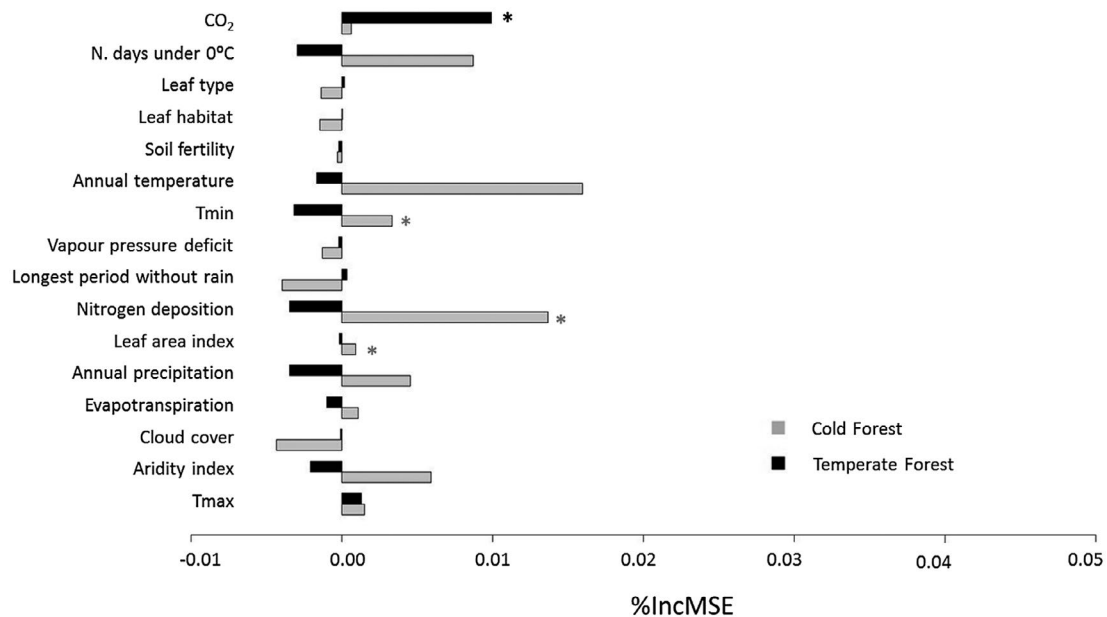


FIGURE 3 Relative importance of vegetation and environmental drivers for maximum radiation use efficiency (RUE_{max}) for cold forests ($n = 20$) and temperate forests ($n = 20$). Data are from (a) random forest analysis (cold forests: light grey bars, temperate forests: black bars) with variable importance positively related to accuracy of model prediction (%IncMSE), and negative %IncMSE indicating lack of importance and (b) univariate analysis, with significant ($p < .10$) drivers marked with "*" symbol (see text and Table 3 for details). Abbreviations: Tmin and Tmax = mean monthly minimum and maximum air temperature, respectively; N. days under 0°C = the number of days in a year with mean daily temperature below 0°C

RUE_{ann} for cold and temperate forests, respectively, and 44 and 88% of the spatial variability of RUE_{max} for cold and temperate forests, respectively. However, note that a high number of variables were retained in the best models (see Tables 2 and 3).

As mentioned above, we also carried out an analysis on the entire data set, without separating forests into the cold and temperate categories. For RUE_{ann} , both temperature-related variables (important for cold forests) and drought-related variables (important for

temperate forests) were significant. Moreover, other variables, significant for at least one of the two forest types, retained their importance (e.g., cloud cover, LAI, N deposition) (Supporting Information Appendix S4). SBRA on the whole data set produced for RUE_{ann} a model with an R^2 (.38, Supporting Information Appendix S4) similar to that for temperate forests (see above). For RUE_{max} , analyses on the entire data set showed only N deposition and LAI having a significant correlation with it (but aridity index presented $p = .08$; Supporting Information Appendix S5) with a clear similarity to the behaviour of cold forests (see Table 3). SBRA on the whole data set produced for RUE_{max} a model with an R^2 (.23, Supporting Information Appendix S5) lower than those obtained for cold and temperate forests separately (see above).

RUE_{max} for cold and temperate forests showed significant interannual variability (Table 4, $SD \pm 0.24$ – 0.30 gC/MJ for both forest types) but, within each forest type, still slightly lower than the spatial variability. Soroe (DK-Sor) forest showed the highest variability in RUE_{max} ($SD \pm 0.45$ gC/MJ, max. 1.66 gC/MJ, min. 0.31 gC/MJ) whereas Loobos (NL-Loo) forest showed the lowest variability ($SD \pm 0.09$ gC/MJ, max. 0.95 gC/MJ, min. 0.58 gC/MJ). For RUE_{ann} , the interannual variability was lower than the interannual variability of RUE_{max} (Table 4, $SD \pm 0.19$ – 0.23 gC/MJ for both forest types). In general, the interannual variability of RUE_{ann} and RUE_{max} was weakly related to the examined variables (Table 5). For RUE_{ann} , for five (out of six) cold forests and three (out of five) temperate forests, interannual variability was not related to any variable. Moreover, the other sites only showed significant relationships with one or two variables per site (variables involved: mainly evapotranspiration and precipitation but also Tmax; see Table 5). For RUE_{max} , significant relationships were found only for three cold forests and one temperate forest. The interannual variability of RUE_{max} was explained mainly by evapotranspiration and precipitation, with some weak relationships ($.05 < p < .10$) with temperature-related variables (see Table 5).

Table 6 and Supporting Information Appendix S8 report the results of the short-term variability analysis of RUE_{8days} for the whole season and for each season separately (i.e., spring, summer, autumn). The variables selected were generally correlated with RUE_{8days} , particularly for cold forests. In fact, for cold forests, RUE_{8days} was significantly correlated with (a) potential evapotranspiration at five sites (out of six), (b) Tmean and Tmin at four sites, and with (c) VPD, annual precipitation and Tmax at about half of the sites. For temperate forests, only three of the five sites presented significant correlations between RUE_{8days} and the examined variables (Table 6). SBRA showed in general R^2 between .21 and .61 (Supporting Information Appendix S9). The low R^2 of some of the SBRA may be related to the fact that important variables were not considered and/or because of nonlinear relationships.

When analysed for the three seasons, cold forests presented two main results. First, cold forests showed the strongest relationships between RUE_{8days} and the environmental factors in summer, for both temperature- and drought-related variables and for all sites. Second, the drivers of RUE_{8days} in spring (mainly VPD, Tmean and Tmin) were different to the drivers of RUE_{8days} in

TABLE 4 Statistics (mean and SD) for interannual variability in annual (RUE_{ann}) and maximum radiation use efficiency (RUE_{max}) in cold and temperate forests. Sites' full names can be found in Supporting Information Appendix S1

Forest type / Site code	N. years	RUE_{ann}		RUE_{max}	
		Mean	SD	Mean	SD
Cold forest					
DE-Hai	8	1.38	± 0.31	1.06	± 0.40
DE-Tha	9	1.39	± 0.21	0.97	± 0.18
DK-Sor	9	1.59	± 0.23	1.18	± 0.45
FI-Hyy	12	0.91	± 0.11	0.81	± 0.36
FI-Sod	8	0.04	± 0.32	0.75	± 0.24
IT-Ren	8	1.02	± 0.22	0.79	± 0.16
Temperate forest					
BE-Bra	10	0.96	± 0.16	0.82	± 0.40
BE-Vie	9	1.59	± 0.20	0.87	± 0.27
FR-Hes	9	1.37	± 0.27	1.16	± 0.27
FR-Pue	8	0.59	± 0.07	0.51	± 0.16
NL-Loo	9	1.21	± 0.23	0.76	± 0.09

autumn (mainly evapotranspiration, Tmax and precipitation) and in any case less relevant (e.g., significant at about half of the sites). For temperate forests, RUE_{8days} appeared to be related to environmental factors mainly in summer and autumn (with dependencies for both temperature- and drought-related variables at most sites) but to be conservative in spring (with only one variable important at one site).

4 | DISCUSSION

One of the main findings of this study is that, on average, cold and temperate forests exhibit very similar RUE_{ann} (c. 1.1 gC/MJ) and RUE_{max} (c. 0.8 gC/MJ) but their relationships with vegetation and environmental drivers differ significantly. Also, the drivers of RUE_{ann} differ from the drivers of RUE_{max} within each forest type. More in detail, RUE_{ann} of cold forests is influenced by mainly variables related to temperature (particularly the number of freezing days), whereas RUE_{ann} of temperate forests by variables related to water status (particularly aridity index). LAI is important for both forest types, whereas cloud cover only for temperate forests and N deposition only for cold forests. On the other hand, RUE_{max} of cold forests was related to LAI and N deposition, whereas RUE_{max} of temperate forests was only weakly related to CO_2 concentration. Concerning the temporal variability, our study shows that interannual variability of RUE_{ann} and RUE_{max} is not primarily related to environmental factors. On the other hand, we showed that short-term (8 days) variability of RUE is strongly related to the environmental conditions, particularly in summer. This evidence was valid for both cold- and temperate forests.

TABLE 5 Results of univariate analysis for interannual variability in annual (RUE_{ann}) and maximum radiation use efficiency (RUE_{max}). The significance level of the linear regression (p) and adjusted R^2 are reported, as well as the sign of the regression. Data are reported for six cold and five temperate forest sites. Sites' full names can be found in Supporting Information Appendix S1

RUE	Potential predictor	Cold forest												Temperate forest											
		DE-Hai		DE-Tha		DK-Sor		FI-Hyy		FI-Sod		IT-Ren		BE-Bra		BE-Vie		FR-Hes		FR-Pue		NL-Loo			
		n	p	n	p	n	p	n	p	n	p	n	p	n	p	n	p	n	p	n	p	n	p		
RUE_{ann}	Precipitation	.66	-.13 (-)	.21	.10 (+)	.61	-.10 (+)	.00**	.85 (+)	.46	-.06 (-)	.97	-.17 (-)	.23	.07 (-)	.01*	.57 (+)	.00**	.77 (+)	.26	.07 (+)	.91	-.14 (+)		
	Evapotranspiration	.57	-.10 (-)	.23	.09 (-)	.47	-.06 (+)	.01*	.53 (-)	.38	-.02 (-)	.28	.06 (+)	.65	-.09 (-)	.00**	.82 (-)	.03*	.42 (-)	.34	.01 (-)	.59	-.09 (+)		
	Vapour pressure deficit	.68	-.13 (-)	.38	-.02 (-)	.38	-.01 (+)	.20	.10 (+)	.80	-.15 (-)	.33	.02 (-)	.14	.16 (+)	.56	-.09 (+)	.67	-.11 (-)	.50	-.07 (+)	.47	-.05 (-)		
	Tmean	.86	-.16 (+)	.10	.25 (-)	.29	.04 (+)	.68	-.10 (-)	.71	-.14 (-)	.23	.10 (-)	.13	.17 (-)	.28	.04 (-)	.15	.17 (-)	.94	-.17 (+)	.78	-.13 (-)		
	Tmin	.88	-.16 (-)	.10	.25 (-)	.32	.02 (+)	.92	-.12	.66	-.13 (+)	.33	.02 (-)	.09°	.24 (-)	.98	-.14 (-)	.35	.00 (-)	.85	-.16 (+)	.47	-.06 (-)		
	Tmax	.47	-.06 (+)	.35	.00 (-)	.24	.07 (+)	.23	.07 (+)	.55	-.10 (-)	.28	.06 (+)	.84	-.12 (-)	.02*	.48 (-)	.31	.02 (-)	.57	-.10 (+)	.68	-.11 (+)		
	CO ₂ concentration	.33	.02 (-)	.91	-.14 (-)	.93	-.14 (-)	.45	-.04 (+)	.52	-.08 (+)	.81	-.15 (-)	.53	-.07 (+)	.27	.05 (+)	.88	-.14 (+)	.61	-.11 (+)	.95	-.14 (+)		
RUE_{max}	Precipitation	.78	-.15 (-)	.68	-.11 (+)	.45	-.05 (+)	.01*	.56 (+)	.80	-.18 (-)	.85	-.16 (+)	.81	-.12 (-)	.03*	.46 (+)	.27	.05 (+)	.87	-.16 (+)	.82	-.13 (+)		
	Evapotranspiration	.03*	.48 (-)	.89	-.14 (-)	.59	-.09 (+)	.04*	.37 (-)	.61	-.13 (+)	.07°	.35 (-)	.46	-.05 (-)	.08°	.29 (-)	.46	-.05 (-)	.27	.06 (-)	.66	-.11 (-)		
	Vapour pressure deficit	.41	-.03 (+)	.55	-.08 (-)	.96	-.14 (+)	.69	-.10 (+)	.76	-.18 (-)	.14	.21 (-)	.07°	.27 (-)	.25	.06 (+)	.84	-.14 (-)	.95	-.17 (-)	.15	.16 (-)		
	Tmean	.96	-.17 (-)	.61	-.10 (-)	.77	-.13 (+)	.39	-.02 (-)	.97	-.20 (+)	.07°	.36 (-)	.06°	.30 (-)	.79	-.13 (-)	.28	.04 (-)	.61	-.11 (-)	.21	.10 (-)		
	Tmin	.32	.02 (+)	.02*	.51 (-)	.73	-.12 (+)	.89	-.12 (-)	.91	-.20 (-)	.10	.28 (+)	.06°	.29 (-)	.35	.00 (+)	.25	.07 (+)	.70	-.14 (-)	.30	.03 (-)		
	Tmax	.70	-.13 (-)	.64	-.11 (+)	.76	-.13 (+)	.08°	.24 (+)	.64	-.14 (+)	.16	.18 (-)	.24	.07 (-)	.17	.15 (-)	.55	-.08 (-)	.87	-.16 (+)	.58	-.09 (-)		
	CO ₂ concentration	.69	-.13 (-)	.76	-.13 (+)	.68	-.11 (-)	.50	-.06 (+)	.03*	.56 (-)	.70	-.14 (+)	.62	-.09 (+)	.25	.07 (+)	.68	-.11 (-)	.19	.14 (+)	.69	-.11 (+)		

Abbreviations and symbols: Tmean = mean temperature; Tmin and Tmax = minimum and maximum air temperature, respectively. ° = .05 < p < .10; * = .01 < p < .05; ** = .001 < p < .001. (+) = positive linear regression; (-) = negative linear regression.

TABLE 6 Results of univariate analysis for short-term variability in radiation use efficiency (RUE_{8days}) of cold and temperate forests, for the whole growing season and spring, summer and autumn separately. Cells in orange are for correlations with $p \leq .05$ and in yellow for correlations with $.05 < p \leq .10$. All detailed data (p and adjusted R^2) are reported in Supporting Information Appendix S8. Data are reported for six cold and five temperate forest sites. Sites' full names and descriptions can be found in Supporting Information Appendix S1

Potential predictor	Cold forest						Temperate forest				
	DE-Hai	DE-Tha	DK-Sor	FI-Hyy	FI-Sod	IT-Ren	BE-Bra	BE-Vie	FR-Hes	FR-Pue	NL-Loo
All seasons											
Tmean		Orange		Orange	Orange			Orange	Orange	Orange	Orange
Tmin	Orange	Orange	Yellow	Orange	Orange			Orange	Orange	Orange	Orange
Tmax		Orange	Orange	Orange	Orange	Orange		Orange	Orange	Orange	Orange
Precipitation		Orange	Yellow	Orange	Orange			Orange	Orange	Orange	Orange
Vapour pressure deficit	Orange			Orange	Orange			Orange	Orange	Orange	Orange
Evapotranspiration	Orange	Orange		Orange	Orange	Orange		Orange	Orange	Orange	Orange
CO ₂ concentration					Orange	Yellow					Orange
SPRING: from mid-April to mid-June											
Tmean	Yellow				Orange						
Tmin	Yellow			Orange	Orange			Orange			
Tmax											
Precipitation		Yellow		Yellow							
Vapour pressure deficit	Orange		Yellow	Orange	Orange		Orange				
Evapotranspiration											
CO ₂ concentration											
SUMMER: from mid-June to mid-August											
Tmean		Orange	Orange	Yellow		Orange		Orange	Orange	Orange	Orange
Tmin		Orange	Yellow			Orange		Orange	Orange	Orange	Orange
Tmax		Orange		Orange				Orange	Yellow	Orange	Orange
Precipitation		Orange	Orange	Orange	Yellow	Yellow	Orange	Orange	Orange	Orange	Orange
Vapour pressure deficit			Orange			Yellow		Orange	Orange	Orange	Orange
Evapotranspiration	Orange	Orange		Orange	Orange		Orange	Orange	Orange	Orange	Orange
CO ₂ concentration				Orange	Orange				Orange	Orange	Orange
AUTUMN: from mid-August to mid-October											
Tmean	Yellow	Orange								Orange	
Tmin							Orange				
Tmax	Orange	Orange						Yellow	Orange	Yellow	Orange
Precipitation	Orange	Orange						Yellow	Orange	Orange	Orange
Vapour pressure deficit							Orange				
Evapotranspiration	Orange	Orange						Orange	Orange	Orange	Orange
CO ₂ concentration		Yellow	Orange		Yellow						

Abbreviations: Tmean = mean temperature; Tmin and Tmax = minimum and maximum air temperature, respectively.

The fact that (low) temperature plays an important role in the eco-physiology of trees in the cold zone is not surprising. Subfreezing temperatures stop photosynthesis, because leaf stomata are forced to close (Waring & Running, 1998). Moreover, negative effects of freezing on RUE could be related to direct frost damage to the leaves (Marchand, 1996) or to indirect, freezing-induced damage to

the hydraulic system that supplies leaves with water and nutrients (e.g., freezing-induced xylem cavitation) (Jackson, Sperry, & Dawson, 2000; Sperry, Nichols, Sullivan, & Eastlack, 1994; Sperry & Sullivan, 1992). Our temporal analysis showed that drought-related variables (e.g., VPD) were also important to determine RUE of cold forests but mainly in summer. Thus, they should not be neglected for seasonal

modelling of RUE but it is also clear that they did not emerge in the annual analyses of either RUE_{ann} or RUE_{max} .

Our results support previous findings that identified drought-related variables (e.g., annual precipitation, aridity index, longest period without rain, VPD) as highly significant determinants of RUE for temperate forests. The negative relationship between drought and RUE in temperate forests is related to the fact that drought impacts on stomatal conductance and restricts the photosynthesis process (e.g., Bracho et al. (2012)). Moreover, in typical drought conditions, a canopy receives more direct light and this has a negative impact on RUE (De Boeck & Verbeeck, 2011). Our temporal analysis for temperate forests showed that temperature-related variables are not to be neglected for short-term modelling of RUE in summer, but as for the case of drought-related variables for cold forests, these variables are not important in the annual analyses of either RUE_{ann} or RUE_{max} .

Both forest types showed relationships with radiation-related variables. The important impact of radiation type (i.e., diffuse versus direct radiation) and radiation interception capacity (i.e., LAI) on photosynthetic efficiency and RUE of forests is well known. Diffuse radiation penetrates deeper in the canopy and does not saturate the photosynthetic capacity at leaf level (Gu et al., 2002). Therefore, greater cloud cover improves the photosynthetic efficiency by decreasing the denominator of Equation 1 at similar values of GPP. Furthermore, more leaves (i.e., higher LAI) correspond to a higher fAPAR.

The key role of nutrient availability in affecting plant and ecosystem processes is well known. In particular, high N availability allows the maintenance of high Rubisco concentration in the leaves, which contributes to a high photosynthetic capacity (Field, Merino, & Mooney, 1983). However, the role of nutrient availability in determining RUE was unclear (Table 1). Our study shows no impact of leaf N or site fertility but a positive impact of N deposition. This indicates the relevance of a fertilization effect, which might be more important than actual N pools (leaf and soil N) and more important in colder (typically nutrient limited) high latitude areas. The past uncertainty in understanding the effect of N deposition on RUE might also have been related to the quality and representativeness of N deposition data. In this work, we used very recent global simulations for N deposition for the period 2004–2006 (Ackerman et al., 2018).

The effect of CO_2 concentration was found to be of some significance but not a key driver of RUE as found by De Kauwe et al. (2016). This might be due to the fact that we analysed natural variability of CO_2 concentration (overall 380 ± 8 ppm) whereas De Kauwe et al. (2016) analysed long-term FACE forest sites with CO_2 concentrations ranging from 370 to 550 ppm. A high CO_2 concentration may increase the effect of CO_2 on RUE.

Our study is difficult to compare to the one of Wang et al. (2017) on a universal mechanism driving RUE across biomes, as the studies are methodologically very different. For instance, our seasonal short-term analysis of RUE variability could have not taken into

account factors found to be important by Wang et al. (2017), such as the ratio of internal leaf CO_2 to external CO_2 , or elevation. On the other hand, both studies found that temperature and a drought-related variable [Wang et al. (2017) considered VPD, we potential evapotranspiration; Table 6] are crucial determinants of the short-term variability of RUE.

Two general remarks should also be made concerning our study. First, the short-term temporal analysis clearly revealed differences among sites, with some sites showing stronger relationships between RUE and the environment than others. This might be the reason why so many contrasting results have been found about the environmental drivers of RUE dynamics in the past (Table 1). Second, one general difficulty in understanding the effects of environmental variables on RUE is finding a good surrogate of each environmental factor at the global scale and their availability at daily to annual time-scales. The accuracy of available meteorological data is of particular importance for modelling the RUE dynamics of ecosystems under stress conditions such as drought. Moreover, note that under drought conditions other specific factors might also play a role as determinants of RUE (Garbulsky et al., 2010; Goerner et al., 2009; Stocker et al., 2018).

In summary, our study synthesized existing knowledge on the determinants of the variability of RUE in cold and temperate forests and tested their potential roles as predictor variables considering a high number of sites in the Northern Hemisphere. We found that, on average, RUE_{ann} and RUE_{max} do not differ markedly between cold and temperate forests, but the influence of different vegetation and environment drivers on RUE does differ significantly between the two climatic zones. These findings primarily indicate that global tools using RUE should differentiate their algorithms between climate zones. For instance, MODIS GPP might improve if current RUE_{max} modulators (temperature, light and VPD) become region-dependent. Also, our study suggests that the use of environmental variables only does not suffice to describe the variability of RUE, and therefore that ecological models based on Monteith's approach should include new parameters that describe plant characteristics such as LAI. N deposition should also be accounted for in modelling RUE of cold forests. Moreover, our results show that, within each climatic zone, RUE_{ann} and RUE_{max} have different relationships with environmental and vegetation variables. Therefore, equations parameterized for one index cannot be used for the other index. Our analysis showed also that RUE_{max} is less related to environmental conditions than RUE_{ann} . This helps modelling and remote sensing applications. In detail, while RUE_{max} for cold forests depends on two variables (LAI and N deposition), RUE_{max} of temperate forests is not related to any variables. So, the latter might be used as a constant. Finally, concerning the temporal variability, our analysis at a short-term scale (i.e. 8-day), indicated that the relationships between RUE and predictors differ when the whole growing season or spring, summer and autumn are considered separately. On the other hand, interannual variability of RUE_{ann} and RUE_{max} was less related to the environment.

ACKNOWLEDGMENTS

IAJ acknowledges the Belgian Science Policy Office (BELSPO) STEREO III program ECOPROPHET (Improved Ecosystem Productivity Modelling by Innovative Algorithms and Remotely Sensed Phenology Indicators) project (SR/00/334). NV and IAJ acknowledge the European Research Council Synergy grant ERC-2013-SyG-610028 IMBALANCE-P. MC was a Postdoctoral Fellow of the Research Foundation – Flanders (FWO). YHF was supported by the University of Beijing Normal University, the General Program of National Nature Science Foundation of China (grant no. 31770516). This work used eddy covariance data acquired by the FLUXNET community and in particular by the following networks: AmeriFlux [U.S. Department of Energy, Biological and Environmental Research, Terrestrial Carbon Program (DE-FG02-04ER63917 and DE-FG02-04ER63911)], AfriFlux, AsiaFlux, CarboAfrica, CarboEuropeIP, CarboItaly, CarboMont, ChinaFlux, Fluxnet-Canada (supported by CFCAS, NSERC, BIOCAP, Environment Canada and NRCAN), GreenGrass, KoFlux, LBA, NECC, OzFlux, TCOS-Siberia, USCCC. We acknowledge the financial support to the eddy covariance data harmonization provided by CarboEuropeIP, FAO-GTOS-TCO, iL-EAPS, Max Planck Institute for Biogeochemistry, National Science Foundation, University of Tuscia, Université Laval and Environment Canada and U.S. Department of Energy and the database development and technical support from Berkeley Water Center, Lawrence Berkeley National Laboratory, Microsoft Research Science, Oak Ridge National Laboratory, University of California – Berkeley, University of Virginia. We gratefully thank all scientists and technicians who helped collect these data and make them available for analysis. We also acknowledge the authors and repository institutions of: Global Forest Database; European Fluxes Database Cluster; 'Global nitrogen deposition (2°×2.5° grid resolution) simulated with GEOS-Chem for 2004-2006' (University of Minnesota); EC-JRC-MARS data set (© European Union, 2011-2014) created by MeteoConsult based on European Centre for Medium-Range Weather Forecasts (ECMWF) model outputs and a reanalysis of ERA-Interim; Global Weather Data for SWAT (<http://globalweather.tamu.edu>); Land and Water Development Division, FAO, Rome, for the Digital Soil Map of the World (<http://www.fao.org/geonetwork>); University of East Anglia Climatic Research Unit (CRU) Time-Series (TS) Version 3.22 for cloud cover data (<http://dx.doi.org/10.5285/18BE23F8-D252-482D-8AF9-5D6A2D40990C>); Land Processes Distributed Active Archive Center (LP DAAC), US Geological Survey (USGS) Earth Resources Observation and Science (EROS) Center (lpdaac.usgs.gov) for providing MODIS data. We thank Erik Fransen (StatUa Center for Statistics, University of Antwerp) for statistic consultancy and Sara Vicca and James Weedon for support on data analysis. This project has received funding from the EU Horizon 2020 Research and Innovation programme under a Marie Skłodowska-Curie grant (INDRO (Remote sensing INDicators for DROught monitoring), grant no. 702717).

CONFLICT OF INTEREST

The authors declare no competing financial interests.

AUTHOR CONTRIBUTION

MB, NV, IAJ and MC conceived the paper; MB performed the analyses; MB, NV and MC wrote the text; YHF gathered cloud cover data; LS gathered soil-type description; all authors contributed substantially to discussions.

DATA AVAILABILITY STATEMENT

A summarized version of the data set is available in Supporting Information Appendix S1. The full data set can be made available by the leading author upon request.

ORCID

Manuela Balzarolo  <https://orcid.org/0000-0002-7888-1501>

Yongshuo H. Fu  <https://orcid.org/0000-0002-9761-5292>

REFERENCES

- Ackerman, D. E., Chen, X., & Millet, D. B. (2018). *Global nitrogen deposition (2°×2.5° grid resolution) simulated with GEOS-Chem for 1984–1986, 1994–1996, 2004–2006, and 2014–2016*. Retrieved from the Data Repository for the University of Minnesota. <https://doi.org/10.13020/D6KX2R>
- Allen, C. B., Will, R. E., McGarvey, R. C., Coyle, D. R., & Coleman, M. D. (2005). Radiation-use efficiency and gas exchange responses to water and nutrient availability in irrigated and fertilized stands of sweetgum and sycamore. *Tree Physiology*, 25, 191–200. <https://doi.org/10.1093/treephys/25.2.191>
- Allen, R. G., Pereira, L. S., Raes, D., & Smith, M. (1998). Crop evapotranspiration-guidelines for computing crop water requirements. *FAO irrigation and drainage paper 56*. Rome, Italy: FAO.
- Alton, P., North, P., & Los, S. (2007). The impact of diffuse sunlight on canopy light-use efficiency, gross photosynthetic product and net ecosystem exchange in three forest biomes. *Global Change Biology*, 13, 776–787. <https://doi.org/10.1111/j.1365-2486.2007.01316.x>
- Baldocchi, D. D. (2018). Must we incorporate soil moisture information when applying light use efficiency models with satellite remote sensing information? *New Phytologist*, 218, 1293–1294. <https://doi.org/10.1111/nph.15176>
- Bracho, R., Starr, G., Gholz, H. L., Martin, T. A., Cropper, W. P., & Loeschner, H. W. (2012). Controls on carbon dynamics by ecosystem structure and climate for southeastern US slash pine plantations. *Ecological Monographs*, 82, 101–128. <https://doi.org/10.1890/11-0587.1>
- Breiman, L. (2001). Random forests. *Machine Learning*, 45, 5–32.
- Campbell, G. S., & Norman, J. M. (1998). *An introduction to environmental biophysics*. New York, USA: Springer Science & Business Media.
- Campoe, O. C., Stape, J. L., Albaugh, T. J., Allen, H. L., Fox, T. R., Rubilar, R., & Binkley, D. (2013). Fertilization and irrigation effects on tree level aboveground net primary production, light interception and light use efficiency in a loblolly pine plantation. *Forest Ecology and Management*, 288, 43–48. <https://doi.org/10.1016/j.foreco.2012.05.026>
- Chasmer, L., McCaughey, H., Barr, A., Black, A., Shashkov, A., Treitz, P., & Zha, T. (2008). Investigating light-use efficiency across a jack pine chronosequence during dry and wet years. *Tree Physiology*, 28, 1395–1406. <https://doi.org/10.1093/treephys/28.9.1395>
- Cheng, Y.-B., Zhang, Q., Lyapustin, A. I., Wang, Y., & Middleton, E. M. (2014). Impacts of light use efficiency and fPAR parameterization on gross primary production modeling. *Agricultural and*

- Forest Meteorology, 189, 187–197. <https://doi.org/10.1016/j.agrfor.2014.01.006>
- Creutzberg, D. (1987) *Description of units of the FAO-UNESCO soil map of the world legend* (ISRIC Report 1987/01). Wageningen, NL. Retrieved from http://www.isric.org/sites/all/modules/pubdnt/pubdntcnt.php?file=/isric/webdocs/docs/ISRIC_Report_1987_01.pdf&nxmlid=332
- De Boeck, H., & Verbeeck, H. (2011). Drought-associated changes in climate and their relevance for ecosystem experiments and models. *Biogeosciences*, 8, 1121–1130. <https://doi.org/10.5194/bg-8-1121-2011>
- De Kauwe, M. G., Keenan, T. F., Medlyn, B. E., Prentice, I. C., & Terrer, C. (2016). Satellite based estimates underestimate the effect of CO₂ fertilization on net primary productivity. *Nature Climate Change*, 6, 892–893.
- Dile, Y. T., & Srinivasan, R. (2014). Evaluation of CFSR climate data for hydrologic prediction in data-scarce watersheds: An application in the Blue Nile River Basin. *Journal of the American Water Resources Association*, 50, 1226–1241. <https://doi.org/10.1111/jawr.12182>
- FAO. (2007). *Digital soil map of the world version 3.6. Land and water development division*. Rome, Italy: FAO. Retrieved from <http://www.fao.org/geonetwork?uuxmlid=446ed430-8383-11db-b9b2-000d939bc5d8>
- Fernández-Martínez, M., Vicca, S., Janssens, I. A., Luysaert, S., Campioli, M., Sardans, J., ... Peñuelas, J. (2014). Spatial variability and controls over biomass stocks, carbon fluxes, and resource-use efficiencies across forest ecosystems. *Trees*, 28, 597–611. <https://doi.org/10.1007/s00468-013-0975-9>
- Field, C., Merino, J., & Mooney, H. A. (1983). Compromises between water-use efficiency and nitrogen-use efficiency in five species of California evergreens. *Oecologia*, 60, 384–389. <https://doi.org/10.1007/BF00376856>
- Field, C. B., Randerson, J. T., & Malmstrom, C. M. (1995). Global net primary production: Combining ecology and remote sensing. *Remote Sensing of Environment*, 51, 74–88.
- Fuka, D. R., Walter, M. T., MacAlister, C., Degaetano, A. T., Steenhuis, T. S., & Easton, Z. M. (2014). Using the Climate Forecast System Reanalysis as weather input data for watershed models. *Hydrological Processes*, 28, 5613–5623. <https://doi.org/10.1002/hyp.10073>
- Garbulsky, M. F., Penuelas, J., Papale, D., Ardo, J., Goulden, M. L., Kiely, G., ... Filella, I. (2010). Patterns and controls of the variability of radiation use efficiency and primary productivity across terrestrial ecosystems. *Global Ecology and Biogeography*, 19, 253–267. <https://doi.org/10.1111/j.1466-8238.2009.00504.x>
- Gitelson, A. A., & Gamon, J. A. (2015). The need for a common basis for defining light-use efficiency: Implications for productivity estimation. *Remote Sensing of Environment*, 156, 196–201. <https://doi.org/10.1016/j.rse.2014.09.017>
- Goerner, A., Reichstein, M., & Rambal, S. (2009). Tracking seasonal drought effects on ecosystemlight use efficiency with satellitebased PRI in a Mediterranean forest. *Remote Sensing of Environment*, 113, 1101–1111. <https://doi.org/10.1016/j.rse.2009.02.001>
- Goudriaan, J., & Van Laar, H. H. (1994). *Modelling potential crop growth processes. Textbook with exercises*. Dordrecht, The Netherlands: Kluwer Academic Publishers.
- Grace, J., Nichol, C., Disney, M., Lewis, P., Quaife, T., & Bowyer, P. (2007). Can we measure terrestrial photosynthesis from space directly, using spectral reflectance and fluorescence? *Global Change Biology*, 13, 1484–1497. <https://doi.org/10.1111/j.1365-2486.2007.01352.x>
- Gu, L., Baldocchi, D., Verma, S. B., Black, T., Vesala, T., Falge, E. M., & Dowty, P. R. (2002). Advantages of diffuse radiation for terrestrial ecosystem productivity. *Journal of Geophysical Research: Atmospheres*, 107.
- Hunt, E. R. Jr (1994). Relationship between woody biomass and PAR conversion efficiency for estimating net primary production from NDVI. *International Journal of Remote Sensing*, 15, 1725–1730.
- Harris, I., & Jones, P. D. (2014). CRU TS3.22: Climatic Research Unit (CRU) Time-Series (TS) version 3.22 of high resolution gridded data of month-by-month variation in climate (Jan. 1901– Dec. 2013). NCAS British Atmospheric Data Centre. Retrieved from <https://catalogue.ceda.ac.uk/uuid/4a6d071383976a5fb24b5b42e28cf28f>
- Jackson, R. B., Sperry, J. S., & Dawson, T. E. (2000). Root water uptake and transport: Using physiological processes in global predictions. *Trends in Plant Science*, 5, 482–488. [https://doi.org/10.1016/S1360-1385\(00\)01766-0](https://doi.org/10.1016/S1360-1385(00)01766-0)
- Jenkins, J. P., Richardson, A. D., Braswell, B. H., Ollinger, S. V., Hollinger, D. Y., & Smith, M. L. (2007). Refining light-use efficiency calculations for a deciduous forest canopy using simultaneous tower-based carbon flux and radiometric measurements. *Agricultural and Forest Meteorology*, 143, 64–79. <https://doi.org/10.1016/j.agrfor.2006.11.008>
- Kergoat, L., Lafont, S., Arneith, A., Le Dantec, V., & Saugier, B. (2008). Nitrogen controls plant canopy light-use efficiency in temperate and boreal ecosystems. *Journal of Geophysical Research: Biogeosciences*, 113, G04017. <https://doi.org/10.1029/2007JG000676>
- King, D. A., Turner, D. P., & Ritts, W. D. (2011). Parameterization of a diagnostic carbon cycle model for continental scale application. *Remote Sensing of Environment*, 115, 1653–1664. <https://doi.org/10.1016/j.rse.2011.02.024>
- Liaw, A., & Wiener, M. (2002). Classification and regression by random Forest. *R News*, 2, 18–22.
- Luysaert, S., Inglima, I., Jung, M., Richardson, A. D., Reichstein, M., Papale, D., ... Janssens, I. A. (2007). CO₂ balance of boreal, temperate, and tropical forests derived from a global database. *Global Change Biology*, 13, 2509–2537.
- Mäkelä, A., Pulkkinen, M., Kolari, P., Lagergren, F., Berbigier, P., Lindroth, A., ... Hari, P. (2008). Developing an empirical model of stand GPP with the LUE approach: Analysis of eddy covariance data at five contrasting conifer sites in Europe. *Global Change Biology*, 14, 92–108.
- Marchand, P. (1996). *Life in the cold: An introduction to winter ecology*. Lebanon, NH: University Press of New England.
- McCallum, I., Wagner, W., Schmulius, C., Shvidenko, A., Obersteiner, M., Fritz, S., & Nilsson, S. (2009). Satellite-based terrestrial production efficiency modeling. *Carbon Balance and Management*, 4. <https://doi.org/10.1186/1750-0680-4-8>
- Monteith, J. (1972). Solar radiation and productivity in tropical ecosystems. *Journal of Applied Ecology*, 9, 747–766. <https://doi.org/10.2307/2401901>
- Myneni, R. B., Hoffman, S., Knyazikhin, Y., Privette, J. L., Glassy, J., Tian, Y., ... Running, S. W. (2002). Global products of vegetation leaf area and fraction absorbed PAR from year one of MODIS data. *Remote Sensing of Environment*, 83, 214–231. [https://doi.org/10.1016/S0034-4257\(02\)00074-3](https://doi.org/10.1016/S0034-4257(02)00074-3)
- Myneni, R. B., Los, S. O., & Asrar, G. (1995). Potential gross primary productivity of terrestrial vegetation from 1982–1990. *Geophysical Research Letters*, 22, 2617–2620. <https://doi.org/10.1029/95GL02562>
- Ollinger, S. V., Richardson, A. D., Martin, M. E., Hollinger, D. Y., Frolking, S. E., Reich, P. B., ... Schmid, H. P. (2008). Canopy nitrogen, carbon assimilation, and albedo in temperate and boreal forests: Functional relations and potential climate feedbacks. *Proceedings of the National Academy of Sciences USA*, 105, 19336–19341. <https://doi.org/10.1073/pnas.0810021105>
- Peel, M. C., Finlayson, B. L., & McMahon, T. A. (2007). Updated world map of the Köppen-Geiger climate classification. *Hydrology and Earth System Sciences*, 11, 1633–1644.
- Peltoniemi, M., Pulkkinen, M., Kolari, P., Duursma, R. A., Montagnani, L., Wharton, S., ... Makela, A. (2012). Does canopy mean nitrogen concentration explain variation in canopy light use efficiency across 14 contrasting forest sites? *Tree Physiology*, 32, 200–218. <https://doi.org/10.1093/treephys/tpr140>

- Penman, H. L. (1948). Natural evaporation from open water, bare soil and grass. *Proceedings of the Royal Society of London Series A, Mathematical and Physical Sciences*, 193, 120–145.
- Prince, S. D., & Goward, S. N. (1995). Global primary production: A remote sensing approach. *Journal of Biogeography*, 22, 815–835.
- R Core Team. (2015). *R: A language and environment for statistical computing*. Vienna, Austria: R Foundation for Statistical Computing. Retrieved from <http://www.r-project.org/>
- Running, S. W., Nemani, R. R., Heinsch, F. A., Zhao, M., Reeves, M., & Hashimoto, H. (2004). A continuous satellite-derived measure of global terrestrial primary production. *BioScience*, 54, 547–560. [https://doi.org/10.1641/0006-3568\(2004\)054\[0547:ACSMO G\]2.0.CO;2](https://doi.org/10.1641/0006-3568(2004)054[0547:ACSMO G]2.0.CO;2)
- Runyon, J., Waring, R. H., Goward, S. N., & Welles, J. M. (1994). Environmental limits on net primary production and light-use efficiency across the Oregon transect. *Ecological Applications*, 4, 226–237.
- Ryan, M. G., Linder, S., Vose, J. M., & Hubbard, R. M. (1994). Dark Respiration of Pines. *Ecological Bulletins*, 43, 50–53.
- Schwalm, C. R., Black, T. A., Arniro, B. D., Arain, M. A., Barr, A. G., Bourque, C. P. A., ... Wofsy, S. C. (2006). Photosynthetic light use efficiency of three biomes across an east-west continental-scale transect in Canada. *Agricultural and Forest Meteorology*, 140, 269–286. <https://doi.org/10.1016/j.agrformet.2006.06.010>
- Sperry, J. S., Nichols, K. L., Sullivan, J. E., & Eastlack, S. E. (1994). Xylem embolism in ring-porous, diffuse-porous, and coniferous trees of northern Utah and interior Alaska. *Ecology*, 75, 1736–1752. <https://doi.org/10.2307/1939633>
- Sperry, J. S., & Sullivan, J. E. (1992). Xylem embolism in response to freeze-thaw cycles and water stress in ring-porous, diffuse-porous, and conifer species. *Plant Physiology*, 100, 605–613. <https://doi.org/10.1104/pp.100.2.605>
- Stocker, B. D., Zscheischler, J., Keenan, T. F., Prentice, I. C., Peñuelas, J., & Seneviratne, S. I. (2018). Quantifying soil moisture impacts on light use efficiency across biomes. *New Phytologist*, 218, 1430–1449. <https://doi.org/10.1111/nph.15123>
- Turner, D. P., Urbanski, S., Bremer, D., Wofsy, S. C., Meyers, T., Gower, S. T., & Gregory, M. (2003). A cross-biome comparison of daily light use efficiency for gross primary production. *Global Change Biology*, 9, 383–395. <https://doi.org/10.1046/j.1365-2486.2003.00573.x>
- Wang, H., Prentice, I., & Davis, T. (2014). Biophysical constraints on gross primary production by the terrestrial biosphere. *Biogeosciences*, 11, 5987–6001. <https://doi.org/10.5194/bg-11-5987-2014>
- Wang, H., Prentice, I. C., Keenan, T. F., Davis, T. W., Wright, I. J., Cornwell, W. K., ... Peng, C. (2017). Towards a universal model for carbon dioxide uptake by plants. *Nature Plants*, 3(9), 734–741. <https://doi.org/10.1038/s41477-017-0006-8>
- Waring, R. H., ... Running, S. W. (1998). *Forest ecosystems, analysis at multiple scales* (2nd ed.). USA: Academic Press.
- Yuan, W., Cai, W., Xia, J., Chen, J., Liu, S., Dong, W., ... Wohlfahrt, G. (2014). Global comparison of light use efficiency models for simulating terrestrial vegetation gross primary production based on the LaThuile database. *Agricultural and Forest Meteorology*, 192–193, 108–120. <https://doi.org/10.1016/j.agrformet.2014.03.007>
- Yuan, W., Liu, S., Zhou, G., Zhou, G., Tieszen, L. L., Baldocchi, D., ... Wofsy, S. C. (2007). Deriving a light use efficiency model from eddy covariance flux data for predicting daily gross primary production across biomes. *Agricultural and Forest Meteorology*, 143, 189–207. <https://doi.org/10.1016/j.agrformet.2006.12.001>
- Zhao, M., Running, S. W., & Nemani, R. R. (2006). Sensitivity of moderate resolution imaging spectroradiometer (MODIS) terrestrial primary production to the accuracy of meteorological reanalyses. *Journal of Geophysical Research-Biogeosciences*, 111, G01002. <https://doi.org/10.1029/2004JG000004>

BIOSKETCH

Manuela Balzarolo is currently a Marie Curie Postdoctoral Research Fellow at Ecological and Forestry Applications Research Centre (CREAF) in Spain. Her research focuses on the analysis of the impact of climate on ecosystem productivity by using remote sensing data.

SUPPORTING INFORMATION

Additional supporting information may be found online in the Supporting Information section at the end of the article.

How to cite this article: Balzarolo M, Valdameri N, Fu YH, Schepers L, Janssens IA, Campioli M. Different determinants of radiation use efficiency in cold and temperate forests. *Global Ecol Biogeogr*. 2019;28:1649–1667. <https://doi.org/10.1111/geb.12985>